

# Discovery of a nearby young brown dwarf binary candidate

A. Reiners<sup>1,\*</sup>, A. Seifahrt<sup>2</sup> and S. Dreizler<sup>1</sup>

<sup>1</sup> Universität Göttingen, Institut für Astrophysik, Friedrich-Hund-Platz 1, D-37077 Göttingen, Germany  
e-mail: Ansgar.Reiners@phys.uni-goettingen.de

<sup>2</sup> Department of Physics, University of California, One Shields Avenue, Davis, CA 95616, USA

Accepted Mar 05, 2010

## ABSTRACT

In near-infrared NaCo observations of the young brown dwarf 2MASS J0041353-562112, we discovered a companion a little less than a magnitude fainter than the primary. The binary candidate has a separation of 143 mas, the spectral types are M6.5 and M9.0 for the two components. Colors and flux ratios are consistent with the components being located at the same distance minimizing the probability of the secondary being a background object. The brown dwarf is known to show Li absorption constraining the age to less than  $\sim 200$  Myr, and it was suspected to show ongoing accretion, indicating an age as low as  $\sim 10$  Myr. We estimate distance and orbital parameters of the binary as a function of age. For an age of 10 Myr, the distance to the system is 50 pc, the orbital period is 126 yr, and the masses of the components are  $\sim 30$  and  $\sim 15 M_{\text{Jup}}$ . The binary brown dwarf fills a so far unoccupied region in the parameters mass and age; it is a valuable new benchmark object for brown dwarf atmospheric and evolutionary models.

**Key words.** stars: low-mass, brown dwarfs – stars: pre-main-sequence – stars: formation – stars: individual: 2MASS J0041353-562112

## 1. Introduction

Very low mass binaries are of particular interest for a number of reasons. First, the binary fraction at very low masses as well as their orbital properties carry important information about the way binaries form (e.g. Close et al. 2003; Burgasser et al. 2007). Second, all components of a multiple system share the same evolutionary history so that a comparison between binary components is free of a number of degeneracies. Finally, binaries offer a model-independent way to determine the mass through measurement of their orbital period. This third point is most important for our understanding of the evolution of low-mass stars and brown dwarfs in particular at young ages where models still have relatively large uncertainties.

The number of very low mass binaries has grown rapidly over the last years. An updated list of binaries with total masses below  $0.2 M_{\odot}$  can be found at [www.vlmbinaries.org](http://www.vlmbinaries.org), this list carries 99 entries as of Jan 2010. Of particular importance are the brown dwarf binaries with independent age constraints because they deliver empirical constraints on brown dwarf evolution models. Furthermore, in order to determine the mass from orbital motion on reasonable timescales, the orbital period should be short enough, and the binaries should not be too far away so that spectroscopic investigation is possible. Usually, young binaries are members of star forming regions that are located at a distance of 100 pc or more, which makes a detailed investigation of low-mass members very difficult. Therefore, young, nearby, low-mass systems are of very great value for our understanding of low-mass star and brown dwarf evolution.

In this paper, we present the discovery of a new very low mass binary, 2MASS 0041353-562112 (hereafter 2M0041), that is nearby and probably very young. The age of 2M0041 is constrained to be lower than  $\sim 200$  Myr by the detection of Li in an optical spectrum (Reiners & Basri 2009). Reiners (2009)

presents evidence for accretion deduced from the intensity and shape of emission lines, in particular  $H\alpha$ . Ongoing accretion would suggest that 2M0041 may even be as young as 10 Myr. Space motion of 2M0041 is consistent with it being a member of the  $\sim 20$  Myr old Tuc-Hor association or the  $\sim 12$  Myr old  $\beta$  Pic association. Unfortunately, the distance to 2M0041 is not yet known because no parallax measurement is available so far. The distance from spectrophotometry would be 17 pc if the object was an old, single field star, but the real distance is of course larger because the young object is more luminous. As long as no parallax is measured for 2M0041, age, mass, and distance are free parameters that can be constrained by measuring the orbital period of the system.

## 2. Data and Analysis

Data were obtained with NaCo, the Nasmyth Adaptive Optics System (NAOS) and Near-Infrared Imager and Spectrograph (CONICA) at ESO's Very Large Telescope (Lenzen et al. 2003; Rousset et al. 2003). Four images were obtained in service mode on August 14, 2009: One image was taken in  $J$ , one in  $H$ , and two images were obtained in  $K_s$ . We obtained ten individual frames, each of them being the average of 3 observations with an individual exposure time of 30 s each. Thus, the total exposure time is 15 min per image. Individual images were jittered using a  $5''$  jitter box, this allowed efficient reduction of the sky background. The adaptive optics system was used with the N90C10 dichroic using 90% of the light for AO and only 10% for the science camera. We chose this option because no bright AO source was available nearby. All observations were carried out at low airmass ( $< 1.3$ ) and good seeing conditions ( $< 0.8''$ ). We used the S13 camera with a field of view of  $14'' \times 14''$  and a pixel scale of 13.2 mas/pix. For our analysis, we use the standard pipeline products that are provided for service mode observations. Data reduction includes dark subtraction, flat fielding, and sky sub-

\* Emmy Noether Fellow

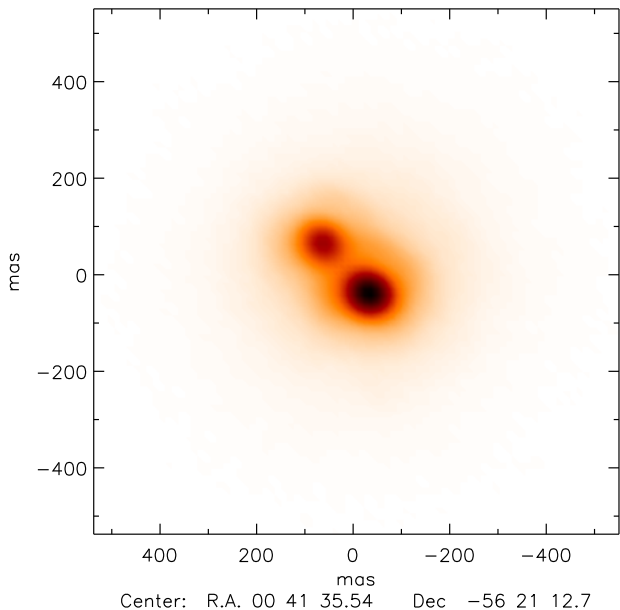


**Fig. 1.** NACO K-band image of 2M0041, North is up and East is left. Axis labels denote coordinates in mas relative to the center of the image.

traction using the jittered images. A close-up of one of the two  $K_s$ -band images is shown in Fig. 1. 2M0041 is clearly resolved as a binary with two components that are somewhat different in brightness; the component to the SW appears brighter than the NE component.

To measure the separation and the flux ratio of the two components, we estimate the PSF from the science images in an iterative procedure. We start with an image of a standard star. We use the so-called zero-point images that are routinely taken for NaCo service observations. With this first guess of the PSF, we search for stars in our science images and determine their position and flux using the public domain IDL package *StarFinder* (Diolaiti et al. 2000). Next, we extract the PSF from the science image given the information on flux and position using the routine `psf_extract` from the *StarFinder* package. We use this PSF in the next step to iteratively search for the two components again and redetermine the shape of the PSF.

The deduction of the PSF from the science image has the advantage that we do not have to rely on a PSF that was taken at a different time, direction, and object brightness. The shape of the PSF sensitively depends on the adaptive optics performance which depends on the brightness of the reference target. On the other hand, the separation of the two components that we wish to distinguish is not much larger than the width of the PSF, particularly in the  $J$ -band. During determination of the PSF, this can lead to the problem that the algorithm constructs a PSF that consists of both components. To avoid this problem, we assume an axisymmetric shape of the PSF. After each PSF determination, we construct a rotationally averaged version of the PSF that we use for the next iteration of *StarFinder*.

We successfully identified the two components in all four images using the procedure described above. As results, we obtain the positions and individual flux of the two components, and the PSF of each image.

We show the separation of the two components, their flux ratio, and the width of the PSF from our four images in Table 1. The results for the separation are consistent with each other. The flux ratios from the two  $K_s$ -band images agree very well, and

**Table 1.** Separation and flux measurements in the four images.

#	Band	Separation [mas]	PA	Flux ratio	PSF width [mas]
1	$J$	142.3	44.90°	$2.19 \pm 0.11$	101.1
2	$H$	142.4	43.34°	$2.06 \pm 0.06$	72.3
3	$K_s$	143.0	43.46°	$1.88 \pm 0.05$	48.2
4	$K_s$	143.4	43.25°	$1.88 \pm 0.05$	52.9

the flux ratio seems to be a function of color, which is consistent with two components of different temperature. The width of the PSF also varies with wavelength, this is expected because the Strehl ratio is lower at shorter wavelengths (Strehl ratios are 0.50 in  $K_s$ , 0.33 in  $H$ , and 0.18 in  $J$ ). Note that in the  $K_s$ -band the width of the PSF is on the order of the diffraction limit. Going to even longer wavelengths would not lead to better image quality because the diffraction limit grows with longer wavelengths (for example, it is  $\sim 100$  mas at  $L'$ ). In the  $J$ -band, the two components are not very well separated. We tried to use a PSF consisting of different elliptical components, but did not succeed to produce results better than our procedure described above. The  $J$ -band position angle differs from the  $H$ - and  $K_s$ -band results by about 1.5 degree, which can be attributed to the slightly irregular shape of the  $J$ -band PSF. In particular, irregularities in the wings of the  $J$ -band PSF may lead to a small shift of the suspected stars' positions (here,  $\lesssim 0.2$  pix or  $\sim 2.5\%$  of the  $J$ -band FWHM). This probably leads to a slight dependence of the photocenter on the stars intensity in the  $J$ -band.

To quantify the uncertainty of our measurements, we performed Monte-Carlo simulations in all three bands. In each band, we constructed a series of 1000 images of a binary consisting of two objects with different flux ratios, separations, and position angles. We uniformly varied these values around those found in the real data, and we used asymmetric PSFs consisting of two elliptical Gaussian components that scatter around a description optimized to fit the rotationally symmetric PSF from the procedure described above. Noise was added to the artificial data in order to match the quality of the real images. In the  $H$ - and  $K$ -bands, the fitting process turned out to be very stable. The clear separation of the two components due to the narrow PSF allows a robust fitting process even in the presence of an asymmetric PSF. We derive the uncertainties in the flux ratio from the scatter around the mean of our simulations. The  $2\sigma$ -scatter of the flux ratio is 3% in  $H$  and 2% in  $K_s$ . The  $J$ -band uncertainties are larger. The main reason is not only the larger FWHM of the PSF, but also the asymmetry in the PSF mentioned above. Thus, the fitting process in the  $J$ -band image sensitively depends on assumptions on the shape of the PSF. Because deconvolving that shape is less reliable in the  $J$ -band image, we decided not to simply adopt the  $J$ -band uncertainties from our Monte-Carlo approach, but conservatively estimate them to be roughly a factor of two larger because of PSF-dependent systematics. We adopt a  $J$ -band flux ratio uncertainty of 5%, which well covers the scatter we found during our attempts using different PSF assumptions.

### 3. Photometry of the components

Photometric measurements of 2M0041 in  $J$ ,  $H$ , and  $K_s$  are available from the Two Micron All Sky Survey (2MASS, Skrutskie et al. 2006). The 2MASS magnitude of 2M0041 reflects the combined flux from both components. With the NaCo

**Table 2.** Measured parameters of the system

Parameter	2MASS A+B	Individual photometry	
		A	B
$J$	$11.96 \pm 0.02$	$12.37 \pm 0.03$	$13.22 \pm 0.04$
$H$	$11.32 \pm 0.02$	$11.75 \pm 0.02$	$12.53 \pm 0.03$
$K_s$	$10.86 \pm 0.03$	$11.32 \pm 0.03$	$12.01 \pm 0.03$
$J - K_s$	$1.10 \pm 0.04$	$1.05 \pm 0.04$	$1.21 \pm 0.05$
$\Delta J$		$0.85 \pm 0.04$	
$\Delta H$		$0.78 \pm 0.02$	
$\Delta K_s$		$0.69 \pm 0.02$	
SpT		$M6.5 \pm 1$	$M9.0 \pm 1$
Position Angle		$43.6^\circ \pm 0.6^\circ$	
Separation [mas]		$142.8 \pm 0.5$	

observations, we can now separate the combined flux into the two components using the 2MASS magnitudes and the flux ratios  $f_1/f_2$  in the three filters; for the  $J$ -band we can write

$$J_2 = J + 2.5 \log \left[ 1 + \left( \frac{f_1}{f_2} \right)_J \right]. \quad (1)$$

The results for individual  $J$ ,  $H$ , and  $K_s$  magnitudes are summarized in Table 2. Under the assumption that the two components are indeed forming a binary (i.e., both are located at the same distance  $d$ ), we can determine the individual spectral types from the magnitude differences and from the information about the combined spectral type from integrated light. Relations between absolute  $J$ -magnitude and Spectral Types were reported by Dahn et al. (2002) and Cruz et al. (2003). The combined spectral type of 2M0041 is M7.5 with an uncertainty of  $\pm 0.5$  (Phan Bao & Bessel 2006). Using the linear relation from Dahn et al. we find that the Spectral Type difference between the two individual components is 2.5 spectral classes. The dispersion of objects around the relation from Dahn et al. is 0.25 mag, which translates into an individual uncertainty of 0.7 spectral classes for individual objects, and an uncertainty of 1.0 spectral classes for the difference between two objects. This dispersion is much larger than the uncertainty from the photometric differences of 2M0041 A and B so that we can neglect the latter.

The linear relation between Spectral Type and absolute magnitude also allows us to use the combined spectral type (M7.5) to anchor the spectral type range of 2M0041 A and B. Using flux ratio and individual magnitudes, we can construct an artificial average magnitude of the combined system 2M0041AB, ( $\tilde{M}_{J,AB} = 12.63$ ,  $\tilde{M}_{K,AB} = 11.55$ ), which in this system must coincide with Spectral Type M7.5  $\pm$  0.5. From that, we derive individual Spectral Types for 2M0041 A and B of M6.5  $\pm$  1.0 and M9.0  $\pm$  1.0, respectively.

An independent check of our assumption that both components are indeed located at the same distance comes from the colors of 2M0041 A and B.  $J-K$  colors of late-M objects are given, e.g., in Hawley et al. (2002), Dahn et al. (2002), and West et al. (2008). The colors of 2M0041 A indicate a spectral type in the range M5–M9 while 2M0041 B falls in the range M8.5–early L. Thus, the colors and flux ratios of 2M0041 A and B support the assumption that both components belong to a binary system: Given a dispersion of 0.2 mag in the  $J-K$  relation and much smaller uncertainties in our measurements of flux ratios and colors, the difference in distance modulus between the two components is unlikely to be larger than 6 pc.

Table 2 also contains the mean position angle and separation. For the position angle, the individual measurements are weighted according to the inverse PSF widths of the images; the result is  $43.6^\circ \pm 0.6^\circ$ . The mean separation calculated from the four exposures is 142.8 mas, we use the scatter of 0.5 mas as a conservative estimate for the uncertainty of this value.

The proper motion of 2M0041 is  $\sim 140 \text{ mas yr}^{-1}$  (Phan Bao & Bessel 2006), i.e., the primary travels roughly by one full observed separation per year in SE direction. The secondary is still bright enough to be visible in archive nIR measurements if the separation to the primary was large enough. We can use nIR or red observations of the region to look whether any signatures of a second object can be found. Assuming that the secondary would show negligible proper motion, the objects should be separated by  $\sim 1.5''$  on the 2 MASS images taken in 1999, which would be difficult to detect given the  $\sim 3''$  FWHM of the 2MASS PSF. On the other hand, ESO.R-MAMA plates taken in 1988 should show two objects separated by about one FWHM, which also is 2.5–3''. We found no second object at the position of 2M0041 in the 2MASS images from 1999 and in the ESO.R-MAMA images from 1988, and we see no signs of an elongated PSF which could be indicative of a barely resolved second object close to the primary ( $\sim 1''$ ). We conclude that it is very likely that the second object in our images is physically bound to the primary. Confirmation of binary status, however, can only be accomplished by verifying common proper motion in an exposure taken at a second epoch.

#### 4. System parameters

From the new photometry, we can determine the parameters of the two components, and we can estimate mass and orbital period for a given age. The distance to 2M0041 can be estimated from the difference between absolute and apparent magnitude. For field objects, the absolute magnitude as a function of spectral type was given by Dahn et al. (2002) and Cruz et al. (2003). We can use that estimate for the lower limit of the distance, which would apply if the objects were field stars. To calculate the distance that would apply if the object was very young, we can then scale the absolute magnitude by the radius difference between young and old objects assuming that the temperature is not significantly changing with age for a given spectral type. We use the radius-age dependence from Baraffe et al. (1998, 2002).

All parameters together with uncertainties are given in Table 3. Uncertainties are due to the spectral type uncertainty, which has an important effect on the absolute magnitude, and to this we add the uncertainty in  $J$  in quadrature. Under the assumption that 2M0041 A is a field star, the distance to the system is 24 pc. As expected, the new distance is larger than the 17 pc calculated earlier (Faherty et al. 2009), because in that calculation, all the flux measured in  $J$  was assumed to come from a single (and cooler) object. We can now use the radius-age relation to estimate the distance for different ages of 2M0041 A (see Reiners 2009). The distances to 2M0041 for ages of 5 and 10 Myr are 71 and 50 pc, respectively. To estimate the semi-major axis, we apply a correction factor of 1.26 to account for projection effects (Fischer & Marcy 1992). The resulting separations between 2M0041 A and B come out as 8.9 and 12.8 AU for a 10 Myr and a 5 Myr binary, respectively.

From the evolutionary tracks of Baraffe et al., we can also estimate the mass of the two components at a given age. With the masses and the separation known, we can then estimate the orbital period of the binary assuming that the distance we observe is the true semimajor-axis of the system.

**Table 3.** System parameters for different ages. The main sequence (MS) case is excluded by the Li detection and given only for reference.

Parameter	Value		
Age [Myr]	5	10	MS
$d$ [pc]	$71^{+29}_{-15}$	$50^{+21}_{-10}$	$24^{+10}_{-5}$
Separation [AU]	$12.8^{+5.3}_{-2.7}$	$8.9^{+3.7}_{-1.9}$	$4.3^{+1.8}_{-0.9}$
Mass (A) [ $M_{\text{Jup}}$ ]	$\sim 25$	$\sim 30$	$\sim 95$
Mass (B) [ $M_{\text{Jup}}$ ]	$\sim 15$	$\sim 15$	$\sim 80$
Orbital Period [yr]	$228^{+155}_{-68}$	$126^{+86}_{-37}$	$22^{+15}_{-7}$

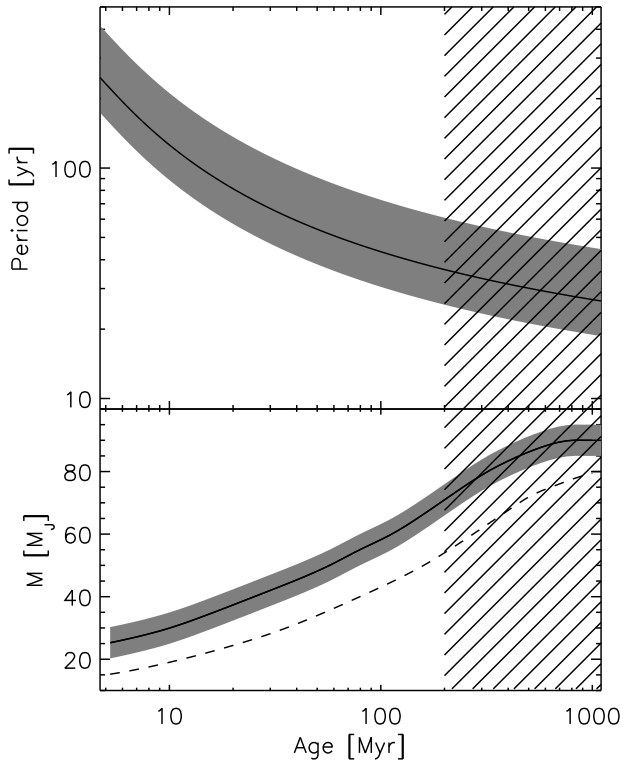


**Fig. 2.** *Top panel:* Estimated orbital period as a function of age for 2M0041A+B (solid line). The grey region indicates  $1\sigma$  uncertainties (see text). *Bottom panel:* Estimated mass as a function of age. The solid line shows the mass of component A, the dashed line is for component B, uncertainties are shown for component A only. The hatched area marks the region excluded from the presence of Li in the spectrum.

The orbital period occurring if the binary was old is  $P \approx 22$  yr. This is the lower boundary for the period, the real period must be longer because an age above a few hundred Myr is excluded by the detection of Li. If 2M0041 has an age of 10 Myr, the period on the order of 126 yr, i.e., a factor of 5 longer. If the system is as young as 5 Myr, the period is about 228 yr, i.e., another factor of two longer. We show the estimated period as a function of age in Fig. 2. With the photometric information gathered about this object, the possible orbital period is a steep function of age.

## 5. Summary

In a NaCo image of the nearby young brown dwarf 2M0041, we have discovered the binarity of this object. The system consists of an M6.5 primary and a secondary of spectral type M9.0. We

find a separation of 143 mas and derive individual  $J$ ,  $H$ , and  $K_s$  magnitudes for both components. Flux ratio and colors of both components are consistent, which means that the chances for the secondary being a background object are very small.

Distance, age, mass, and orbital period are yet unknown, but we can present possible solutions as a function of age. The object still has lithium, which means that it is a brown dwarf younger than a few hundred Myr.  $H\alpha$  and other optical emission lines indicate that the object may be accreting so that its age may be as low as 10 Myr. For this age, the period is predicted to be on the order of 125 yr at a separation of  $\sim 9$  AU and a distance of 50 pc. Age, semi-major axis, and distance are steep functions of the orbital period. So far, no parallax measurement is available so that the distance to the binary is unknown given that we do not certainly know its age.

Objects of spectral type M9.0 are much fainter at optical wavelengths than M6.5 so that the secondary contributes negligible background continuum to the  $H\alpha$  and Li measurement. On the other hand, the  $H\alpha$  emission seen in the combined spectrum may come from either of the two components, or both, which would affect the measured accretion rate; if both objects are accreting, the accretion rate per star would be lower, but the shape and strength of  $H\alpha$  still would indicate accretion. Alternatively, if the accretion timescale is longer on the secondary, it may be the only accreting object in the system. In that case, the accretion rate would be higher than the one originally derived. An image taken at  $H\alpha$  or even spatially resolved spectroscopy can solve this issue.

The discovery of binarity in this young brown dwarf opens the opportunity to directly determine the mass of two young nearby brown dwarfs that may be accreting. Without knowing the distance, the age of the system can be determined from the orbital period. In the next years, the first estimate of the orbital period will become available. If it is indeed as young as a few ten Million years, it is the first object in this mass/age regime for which a direct mass estimate will become available. With a measured parallax, independent information on the distance putting strong constraints on the system's parameters will be given. This system will be an important benchmark for brown dwarf evolutionary models at young ages.

**Acknowledgements.** We thank an anonymous referee for a very helpful report. Based on observations made with the European Southern Observatory, PID 383.C0708. This publication has made use of the Very-Low-Mass Binaries Archive housed at <http://www.vlmbinaries.org> and maintained by Nick Siegler, Chris Gelino, and Adam Burgasser. A.R. acknowledges research funding from the DFG as an Emmy Noether fellow under RE 1664/4-1, AS acknowledges financial support from NSF grant AST07-08074.

## References

- Baraffe, I., Chabrier, G., Allard, F. & Hauschildt, P.H., 1998, A&A, 337, 403
- Baraffe, I., Chabrier, G., Allard, F. & Hauschildt, P.H., 2002, A&A, 382, 563
- Burgasser, A. J., Reid, I. N., Siegler, N., Close, L., Allen, P., Lowrance, P., & Gizis, J. 2007, Protostars and Planets V, arXiv:astro-ph/0602122
- Close, L.M., Siegler, N., Freed, M., & Biller, B., 2003, ApJ, 587, 407
- Dahn, C.C., Harris, H.C., Vrba, F.J., Guetter, H.H., et al., 2002, ApJ, 124, 1170
- Cruz, K.L., Reid, I.N., Liebert, J., Kirkpatrick, J.D., & Lowrance, P.J., 2003, AJ, 126, 2421
- Diolaiti, E., Bendinelli, O., Bonaccini, D., Close, L., Currie, D., & Parmeggiani, G., 2000, A&AS, 147, 335
- Faherty, J.K. et al., 2009, AJ, 137, 1
- Fischer, D.A., & Marcy, G.W., 1992, ApJ, 396, 178
- Hawley, S.L., Covey, K.R., Knapp, G.R., Golimowski, D.A., et al., 2002, ApJ, 123, 3409
- Lenzen, R. et al., 2003, SPIE 4841, 944
- Phan Bao, N., Bessel, M.S., 2006, A&A, 515, 523
- Reiners, A., 2009, ApJ, 702, L119

- Reiners, A., & Basri, G., 2009, *ApJ*, 705, 1416
- Rousset, G. et al. 2003, *SPIE* 4839, 140
- Skrutskie, M.F., Cutri, R.M., Stiening, R., Weinberg, M.D., Schneider, S., Carpenter, J.M., et al., 2006, *AJ*, 131, 1163
- West, A.A., Hawley, S.L., Bochanski, J.J., Covey, K.R., Reid, N.L., Dhital, S., Hilton, E.J., & Masuda, M., 2008, *ApJ*, 135, 785